ONCOIMMUNOLOGY
2017, VOL. 6, NO. 3, e1278331 (10 pages)
http://dx.doi.org/10.1080/2162402X.2016.1278331

Taylor & Francis
Taylor & Francis Group

ORIGINAL RESEARCH

IL4-induced gene 1 promotes tumor growth by shaping the immune microenvironment in melanoma

Lloyd Bod[a,b,c], Renée Lengagne[a,b,c], Ludovic Wrobel[d], Jan Philipp Ramspott[a,b,c], Masashi Kato[e], Marie-Françoise Avril[a,b,c,f], Flavia Castellano[g,h,i], Valérie Molinier-Frenkel[g,h,j], and Armelle Prévost-Blondel[a,b,c]

[a]Inserm, U1016, Institut Cochin, Paris, France; [b]Cnrs, UMR8104, Paris, France; [c]Université Paris Descartes, Sorbonne Paris Cité, Paris, France; [d]Hôpitaux Universitaires de Genève, Genève, Switzerland; [e]Nagoya University Graduate School of Medicine, Nagoya, Aichi, Japan; [f]APHP, Hôpital Cochin, Paris, France; [g]INSERM, U955, Equipe 09, Créteil, France; [h]Université Paris Est, Faculté de Médecine, Créteil, France; [i]AP-HP, Hôpital H. Mondor - A. Chenevier, Plateforme de Ressources Biologiques, Créteil, France; [j]AP-HP, Hôpital H. Mondor - A. Chenevier, Service d'Immunologie Biologique, Créteil, France

ABSTRACT

Amino acid catabolizing enzymes emerged as a crucial mechanism used by tumors to dampen immune responses. The L-phenylalanine oxidase IL-4 induced gene 1 (IL4I1) is expressed by tumor-associated myeloid cells of most solid tumors, including melanoma. We previously provided the only evidence that IL4I1 accelerates tumor growth by limiting the $CD8^+$ T cell mediated immune response, in a mouse model of melanoma cell transplantation. Here, we explored the role of IL4I1 in Ret mice, a spontaneous model of melanoma. We found that IL4I1 was expressed by $CD11b^+$ myeloid cells and that its activity correlated with disease aggressiveness. IL4I1 did not enhance tumor cell proliferation or angiogenesis, but orchestrated the remodeling of the immune compartment within the primary tumor. Indeed, the inactivation of IL4I1 limited the recruitment of polymorphonuclear myeloid-derived suppressor cells and enhanced the infiltration by Th1 and cytotoxic T cells, thus delaying tumor development and metastatic dissemination. Accordingly, human primary melanomas that were poorly infiltrated by $IL4I1^+$ cells exhibited a higher density of $CD8^+$ T cells. Collectively, our findings strengthen the rationale for therapeutic targeting of IL4I1 as one of the key immune regulators.

ARTICLE HISTORY
Received 22 November 2016
Revised 21 December 2016
Accepted 28 December 2016

KEYWORDS
$CD8^+$ T cells; IL4I1; primary melanoma; tumor escape

Introduction

Emerging data highlight the key role of amino-acid metabolizing enzymes (e.g. arginase 1, inducible nitric oxide synthase and indoleamine-2,3-dioxygenase) in tumor escape from immunosurveillance.[1] Among those, the secreted IL4I1 (interleukin-4-induced gene 1) enzyme catabolizes L-phenylalanine and to a lesser extent arginine to generate hydrogen peroxide (H_2O_2), ammonia (NH_3) and the corresponding α-keto acid. In cancer patients, IL4I1 is expressed either by tumor cells themselves (e.g., some B cell lymphoma subsets, mesothelioma or ovarian cancer) or by tumor-associated macrophages or dendritic cells (DC).[2,3] Its expression in stromal cells has been associated with a poor outcome in breast cancer.[4]

IL4I1 exerts several immunoregulatory properties *in vitro*, mainly on T lymphocytes.[5] Indeed, it inhibits *in vitro* the proliferation of effector/memory T cells and decreases the production of inflammatory chemokines and Th1 cytokines (IFNγ and IL2).[6,7] The mechanisms involved may comprise direct downregulation of the expression of the CD3ζ chain through H_2O_2 production[6] and/or indirect inhibition *via* stimulation of naive $CD4^+$ T cell differentiation into regulatory T cells (Treg)[8] or *via* macrophage polarization toward an M2 phenotype.[9] IL4I1 also limits TCR-mediated expansion of T helper type 17 (Th17) by preventing their entry into cell cycle.[10] We provided the first—and to our knowledge unique—evidence that transplantation of B16-F10 melanoma cells transfected with a murine IL4I1 cDNA inhibits the development of the antitumor $CD8^+$ T cell response, concomitantly facilitating tumor growth. The IL4I1 enzymatic activity leading to the impairment of tumor specific T cell functions and subsequent tumor outgrowth in this model were close to those detected in human primary melanoma, a tumor where the IL4I1 activity is supported exclusively by tumor-associated macrophages. These data strongly suggested the role of this enzyme in tumor escape from the immune surveillance.[11] Nevertheless, the impact of IL4I1 on the tumor microenvironment in the course of tumor development remains to be clarified.

Here, we used a murine model of spontaneous melanoma to directly investigate the influence of the genetic inactivation of IL4I1 during tumor development and immune escape. Ret mice constitutively express the proto-oncogene c-ret.[12] They develop a primary uveal tumor at three weeks of age that disseminates rapidly through the skin and later through distant organs.[13-15] In the present study, we demonstrate that IL4I1 expression contributes to the tumor progression by promoting the recruitment of myeloid cell subsets and by interfering with the antitumor properties of T lymphocytes within the primary

CONTACT Armelle Prévost-Blondel armelle.blondel@inserm.fr Cochin Institute, 75014, Paris, France.
Supplemental data for this article can be accessed on the publisher's website.

tumor. We also report an inverse relationship between the density of IL4I1^{+} cells and CD8^{+} T cells in primary tumors from melanoma patients.

Results

IL4I1 activity correlates with melanoma progression in Ret mice

To determine whether IL4I1 was detected in the Ret model, we measured its specific enzymatic activity in protein lysates from the spleen and cervical lymph nodes (cervLN) draining the primary tumor. We measured IL4I1 activity by quantifying L-phenylalanine oxidation, as described previously.[2,6] IL4I1 activity was similar in cervLN of Ret and wild-type (WT) mice, whereas it was increased by 2-fold in spleen from Ret mice (Fig. 1A). This activity was even higher in animals with distant metastasis and positively correlated with melanoma progression (Fig. 1B). Next, we purified CD11b^{+} or CD11b^{-} splenocytes from animals exhibiting distant metastasis and observed that the IL4I1 transcript was mainly expressed by CD11b^{+} myeloid cells (Fig. 1C). Interestingly, the level of IL4I1 transcripts positively correlated with arginase 1 level, but not iNOS level in splenic CD11b^{+} cells (Fig. S1). At the primary tumor site, IL4I1 activity was restricted to the haematopoietic compartment (Fig. 1D) and its transcript was mostly detected in tumor infiltrating CD11b^{+} cells (Fig. 1E). Collectively, these results suggest that, in our model, myeloid cells are the main producers of IL4I1 and IL4I1 activity is associated with melanoma aggressiveness.

The genetic inactivation of IL4I1 delays the tumor development in Ret mice

To further understand the role of IL4I1 expressed by myeloid cells during melanoma progression, Ret mice were bred with IL4I1-deficient animals to derive Ret$^{+/-}$ IL4I1$^{-/-}$ (RetIL4I1KO) mice. Starting at weaning, these mice and their littermates were monitored for the occurrence of primary tumor and cutaneous metastasis. Three-month-old mice were killed and analyzed for the presence of internal metastasis, distant from the uveal melanoma. Fifty percent of RetIL4I1KO mice had a primary tumor at day 48, whereas the median time for tumor detection in Ret mice was day 33 (Fig. 2A). Although the development of the primary tumor was significantly delayed, it still occurred in more than 90% of 3 mo old RetIL4I1KO mice. In addition, IL4I1 deficiency delayed the tumor cell dissemination at facial (Fig. 2B) and back sites (Fig. 2C) as well as more distant sites, mainly bladder or mediastinal lymph nodes observed at the autopsy (Fig. 2D). The onset of vitiligo-like depigmentation, which is associated with a better outcome in the Ret model,[15] was similar in both groups (Fig. 2E). The pro-tumor properties of IL4I1 were confirmed in the B16-F10 melanoma model. Indeed, the tumor growth of B16-F10 cells transplanted subcutaneously was delayed in IL4I1KO mice when compared with WT mice, and their volumes were smaller (Fig. S2A). After intravenous melanoma cell injection, IL4I1KO mice also exhibited 6-fold less lung foci than aged matched WT mice (Fig. S2B). These results are consistent with IL4I1 effect on metastatic dissemination observed in the Ret model.

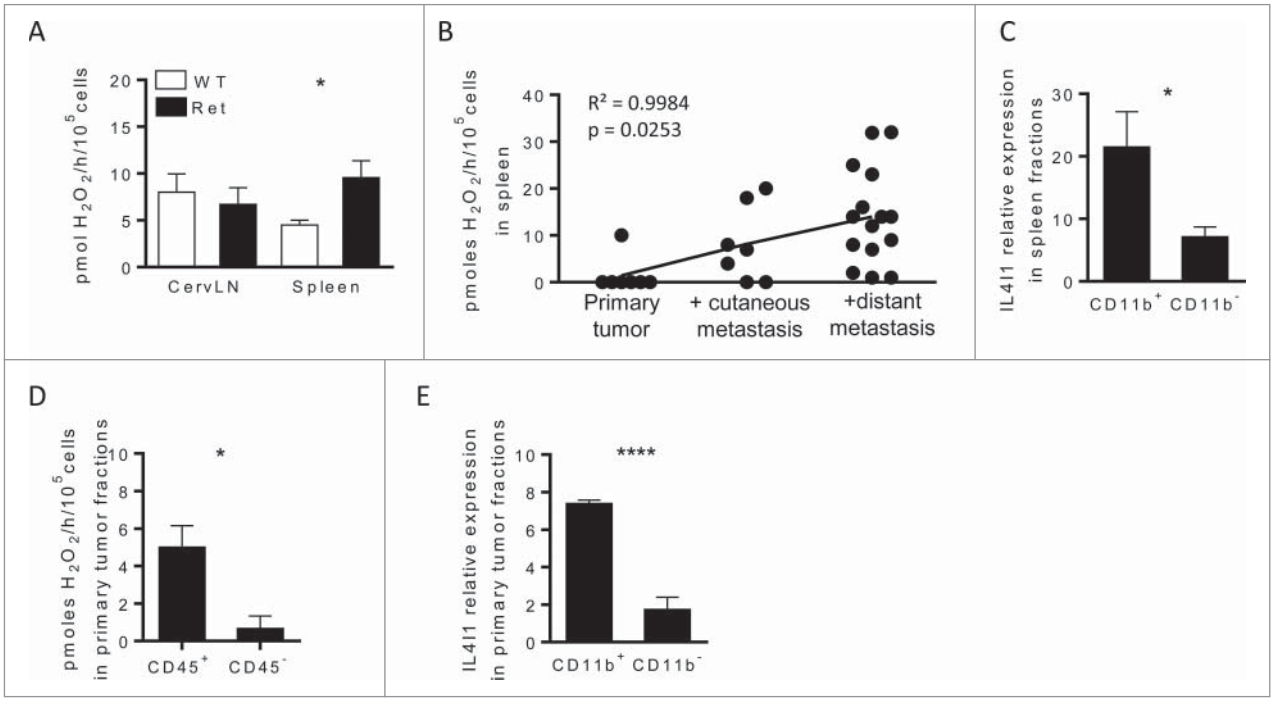

Figure 1. IL4I1 is mainly expressed by myeloid cells and correlates with disease progression in Ret mice (A and D) IL4I1 activity in cervLN, spleen (A) or tumor fractions (D) from WT (white) or Ret (black) mice. (B) Pearson correlation of IL4I1 activity from spleen of Ret mice depending on the tumor stage. (C and E) IL4I1 expression was measured by qRT-PCR in purified CD11b^{+} or CD11b^{-} fractions isolated from spleen (C) or primary tumors (E) of Ret mice. Experiments were performed from Ret mice at different stages of melanoma development (A and B), or from 3 to 6-mo old mice exhibiting distant metastasis, respectively (C–E). Data were pooled from at least three independent experiments. $^{*}p < 0.05$; $^{****}p < 0.0001$.

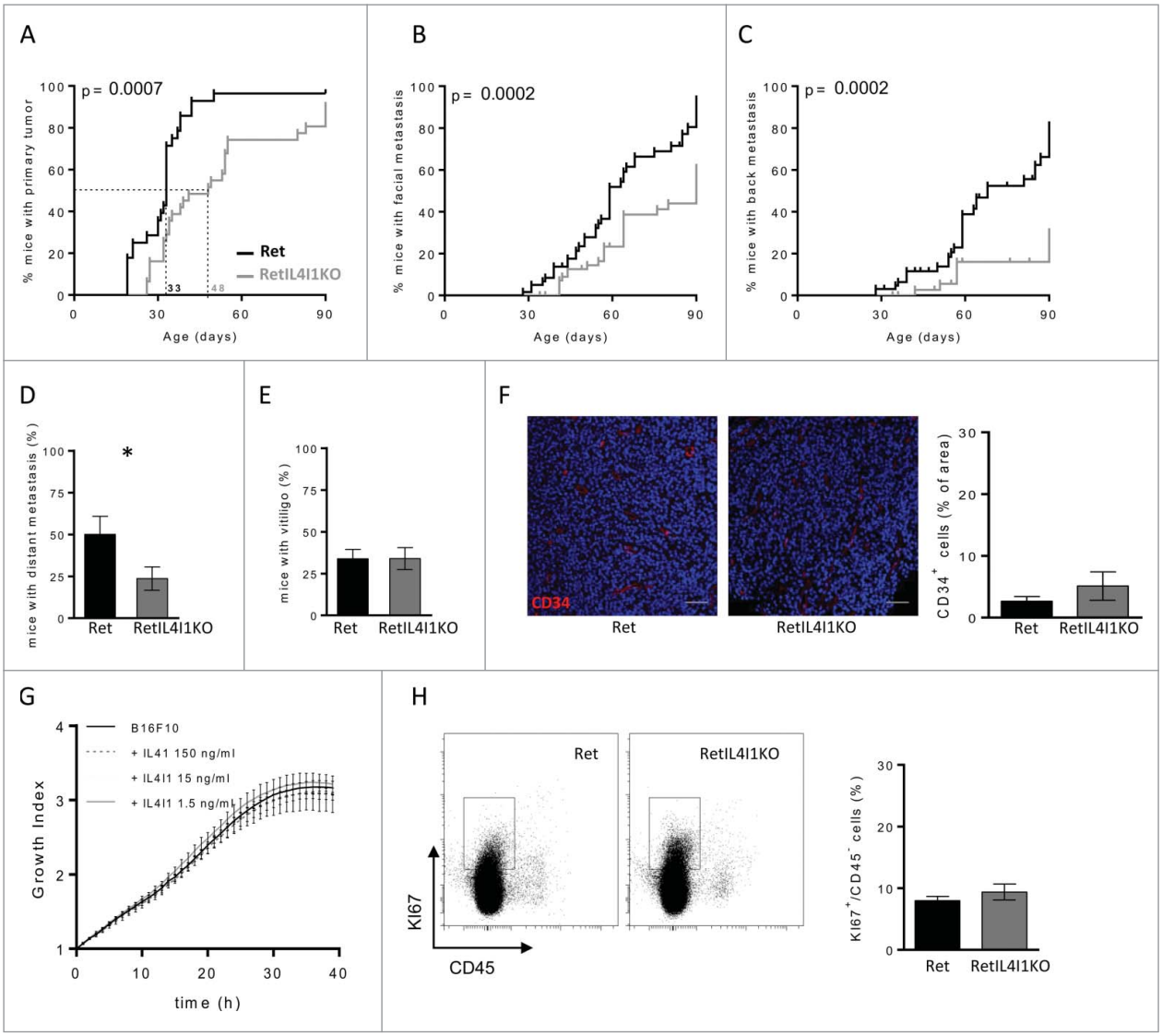

Figure 2. IL4I1 favors melanoma progression and metastasis formation with no direct effect on tumor cell proliferation and angiogenesis. (A–E) Melanoma progression in Ret (black line, $n = 28$) or RetIL4I1KO (gray line, $n = 32$) mice was evaluated once a week over a 3-mo period. Time courses of primary tumor (A), facial (B) or dorsal (C) metastasis onset. Frequency of 3-mo old mice with distant metastasis (D) or vitiligo (E) are shown. Mantel-Cox test (A–C). (F) Illustration and quantification of the CD34 vessel staining in primary tumors of 3-mo old Ret or RetIL4I1KO mice. Scale bar, 100 μm. (G) Growth comparison of B16-F10 cells seeded in E-plates wells with or without recombinant IL4I1. (H) Proportion of KI67$^+$ cells among CD45$^-$ cells within the primary tumors of 3-mo old Ret and RetIL4I1KO mice. Data were pooled from at least three experiments. $^*p < 0.05$.

To explain these observations, we first wondered whether IL4I1 may promote angiogenesis. However, intra-tumor vessel density assessed by CD34 staining was similar within the primary tumors of 3 mo old Ret and RetIL4I1KO mice (Fig. 2F). We next assessed whether IL4I1 directly enhanced the tumor cell proliferation, by monitoring the proliferative index of B16-F10 cells cultured up to 40 h in the presence of increasing doses of recombinant IL4I1. As shown in Fig. 2G, even at a high dose (150 ng mL^{-1}), IL4I1 did not accelerate the growth of B16-F10 cells *in vitro*. In line with this result, proliferating KI67$^+$ tumor cells assessed *ex vivo* by flow cytometry were as frequent in RetIL4I1KO mice as in Ret mice at the autopsy (Fig. 2H). Together, these findings indicate that the rapid metastatic spreading in Ret mice may not depend on IL4I1 direct effect on tumor cells themselves or their vascularization.

The inactivation of IL4I1 limits myeloid cell recruitment and favors B and T cell accumulation at the primary tumor site

To decipher if IL4I1 favors metastatic dissemination by modifying the immune microenvironment of tumor cells, we studied by flow cytometry the myeloid and lymphoid subsets within primary tumors from 3 mo old Ret mice. Whereas IL4I1 deficiency did not affect the global CD45$^+$ cell infiltrate (Fig. 3A), both the myeloid and lymphoid compartments among CD45$^+$ cells were drastically modified (Fig. 3B and Table 1). Indeed, primary tumors from RetIL4I1KO mice exhibited significantly less myeloid cells than those from aged matched Ret mice (44.6% vs. 59.3% and 7.6×10^4 cells vs. 140×10^4 cells) (Fig. 3C). The proportions and numbers of DC (CD11c$^+$) and monocytic myeloid-derived suppressor cells (M-MDSC, Ly6C^{high} Ly6G$^-$)

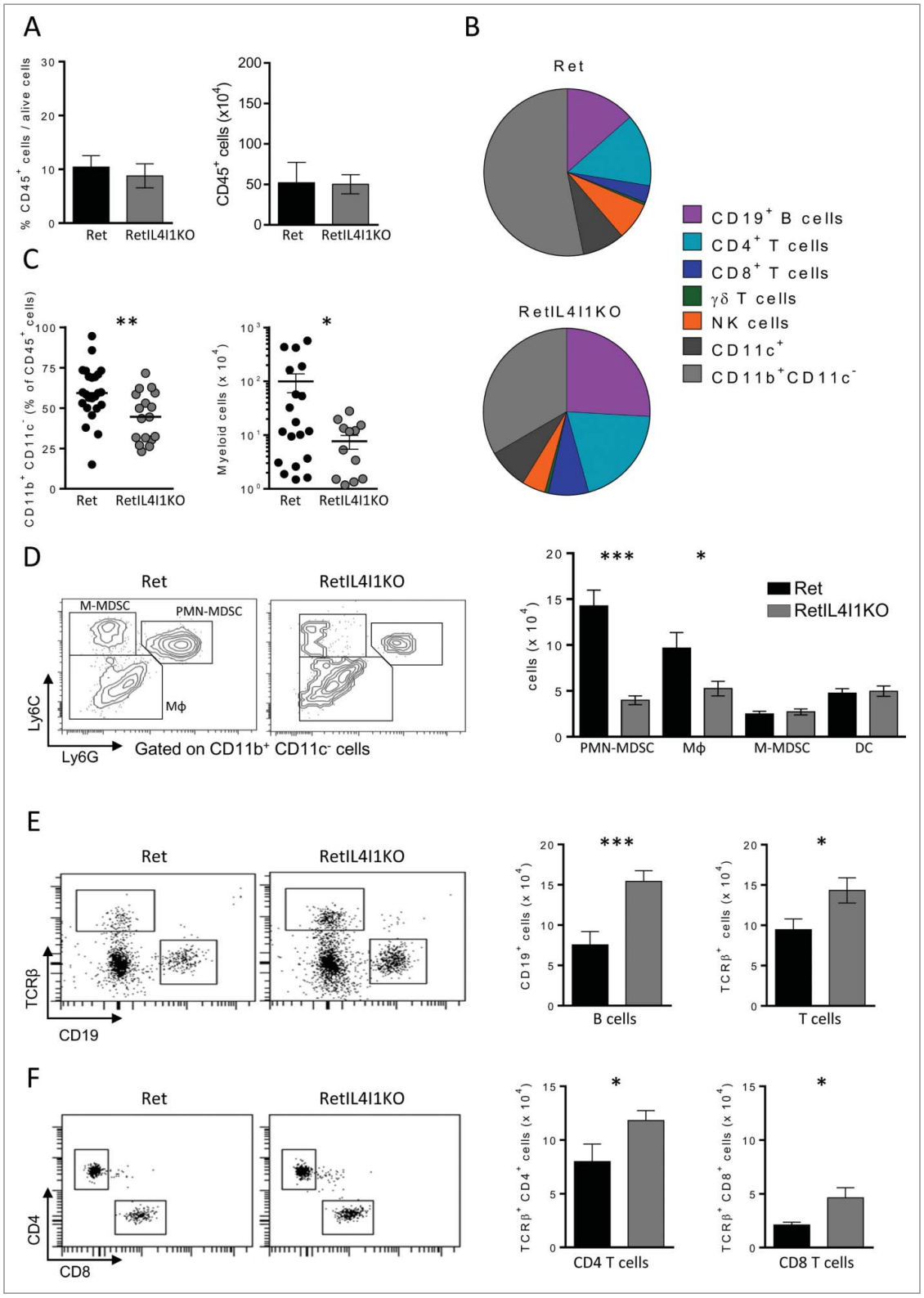

Figure 3. Remodeling of immune cell infiltration in primary tumor of mice lacking IL4I1. (A) Proportions and absolute numbers of $CD45^+$ cells within primary tumors of 3-mo old Ret and RetIL4I1KO mice. (B) Distribution of immune cells infiltrating Ret (top) and RetIL4I1KO (low) primary tumors. (C) Proportion and absolute numbers of myeloid cells. (D–F) Absolute numbers of DC ($CD11c^+$), MΦ ($CD11b^+CD11c^-Ly6C^{-/low}Ly6G^-$), M-MDSC ($CD11b^+CD11c^-Ly6C^{high}Ly6G^-$) and PMN-MDSC ($CD11b^+CD11c^-Ly6C^{int}Ly6G^+$) (D) and also $CD19^+$ B cells and TCR^+ cells (E) subdivided into $CD4^+$ or $CD8^+$ T cells (F). Representative gating strategies are shown (D, E, F; left). Data are pooled of at least three independent experiments. Mean and SEM. $^*p < 0.05$; $^{**}p < 0.01$; $^{***}p < 0.001$.

were not significantly modulated by IL4I1 inactivation (Fig. 3D and S3A). In contrast, polymorphonuclear myeloid-derived suppressor cells (PMN-MDSC, $Ly6C^{int}$ $Ly6G^+$) and macrophages ($Ly6C^{-/low}$ $Ly6G^-$) poorly infiltrated primary tumors in RetIL4I1KO mice compared with Ret mice (Fig. 3D and S3A). Regarding the lymphoid infiltrate, while the amount

Table 1. Quantification of immune populations infiltrating the primary tumor (%).

Cell populations	Ret mice	RetIL4I1KO mice	*p*-values
CD11b+CD11c-Ly6G+Ly6Cint	28.05 ± 11.02	7.94 ± 3.86	< 0.0001
CD11b+CD11c-Ly6G-Ly6Clow/−	18.57 ± 8.64	10.48 ± 5.46	0.0221
CD11b+CD11c-Ly6G-Ly6Chigh	4.79 ± 2.26	5.41 ± 2.44	ns (0.4788)
CD11c+	8.82 ± 3.9	9.34 ± 4.03	ns (0.7028)
TCRβ+ CD4+	15.09 ± 11.64	23.55 ± 7.34	0.0212
TCRβ+CD8+	3.54 ± 1.89	9.24 ± 5.61	0.0154
TCR$\gamma\delta$+	0.58 ± 0.20	0.87 ± 0.44	ns (0.094)
TCRβ-NK1.1+	7.83 ± 5.13	5.39 ± 2.66	ns (0.1223)
CD19+	14.53 ± 13.77	30.77 ± 14.9	0.0003

ns: non-significant

of $\gamma\delta$ T cells and NK cells was not modified by the absence of IL4I1, tumor infiltrating B lymphocytes, $CD4^+$ and $CD8^+$ T lymphocytes were more numerous in RetIL4I1KO mice (Fig. 3E–F and S3B–C). On the other hand, no significant difference between Ret and RetIL4I1KO mice was found in the proportion of immune cells measured in the spleen and tumor draining lymph node (Fig. S4A). These data indicate that the presence of IL4I1 promotes the accumulation of PMN-MDSC and macrophages at the tumor site, while limiting the B and T cell infiltrate. These modifications of the immune microenvironment may be responsible for the observed enhanced tumor progression in Ret mice.

T cells infiltrating IL4I1-deficient primary tumors exhibit antitumor properties

As IL4I1 is known for its T cell inhibition properties, we assessed the impact of IL4I1 inactivation on the functions of tumor infiltrating B and T lymphocytes. First, we evaluated the production of tumor-specific antibodies in the sera of Ret and RetIL4I1KO mice. For this purpose, sera were incubated either with a tumor cell line derived from a Ret mouse metastasis (Melan-Ret) or with a control lymphoma cell line (H9), before revelation by a fluorescent secondary antibody and flow cytometry analysis. Specific staining revealed the presence of tumor-reactive antibodies only against Melan-Ret cells. Sera of RetIL4I1KO (13 out of 17) and Ret (15 out of 22) mice similarly recognized melanoma cells, indicating that tumor specific antibodies are not increased in mice lacking IL4I1 (Fig. 4A). In agreement with this, the proportion of plasma cells ($CD138^+$ $B220^{low}$) in lymphoid organs was similar in both mice (Fig. S4B).

We next evaluated *ex-vivo* the functional status of $CD4^+$ and $CD8^+$ T cells isolated from the primary tumors of Ret and RetIL4I1 KO mice. Higher proportions of $CD4^+$ T cells expressing the proliferation-related Ki-67 antigen or producing IFNγ were detected in RetIL4I1KO mice (Fig. 4B and 4C). While the proportion of $CD8^+$ T cells expressing Ki67 was similar in both groups (Fig. 4D), their capacity to produce IFNγ was increased in the absence of IL4I1 (Fig. 4E), as was their cytotoxic capacity evaluated by extracellular exposure of the lytic granule marker CD107a (Fig. 4F). Increased levels of IL-12 in the sera of RetIL4I1KO mice accompanied this T cell profile (Fig. S4C). Finally, the proportion of peripheral Treg ($TCR\beta^+$ $CD4^+$ $FOXP3^+$) seemed unaffected by IL4I1 deficiency (Fig. S4D). Altogether, our results suggest that the inactivation of IL4I1 stimulates antitumor immunity in primary tumors by decreasing myeloid cell infiltration while inducing a more potent T helper type 1 and cytotoxic T cell response.

IL4I1 overexpressing tumors are poorly infiltrated in $CD8^+$ T cells in melanoma patients

The above results suggest that IL4I1 inactivation represent a therapeutic strategy to revitalize the antitumor immune response of melanoma patients. To evaluate if the mouse results are pertinent in the human situation, we examined the relationship between the density of $IL4I1^+$ cells and the presence of $CD8^+$ T cells in human melanoma biopsies. $CD8^+$ and IL4I1 stainings were performed on primary tumors from 20 melanoma patients (see Table 2 for patient's characteristics). We observed tumors displaying different levels of IL4I1 expression with an average median of 22 $IL4I1^+$ cells mm^{-2} as illustrated in Fig. 5A. Interestingly, tumors with more than 22 $IL4I1^+$ cells mm^{-2} exhibited a significantly lower density of $CD8^+$ T cells (Fig. 5B). These results suggest that the local IL4I1 expression limits the $CD8^+$ T cell infiltrate.

Discussion

Tumors use multiple suppressive strategies to escape from antitumor immune responses, in particular, they favor the expression of enzymes which affect amino acid catabolism, such as IL4I1.[1,16] In the present study, we investigated the role of the IL4I1 phenylalanine oxidase in the context of the spontaneous development of a metastatic melanoma. We show that in the primary tumor of Ret mice, IL4I1 expression is mainly restricted to the myeloid compartment and augments during tumor progression.

The role of myeloid cells in tumor development has been widely described.[27-29] Tumor infiltrating myeloid cells are known to express high levels of arginase 1, another amino acid consuming enzyme, that contributes to their suppressive activity.[17] In the Ret model, we have previously reported that splenic or tumor derived myeloid cells express arginase 1.[18] Here, we further reveal that IL4I1 expression positively correlates with arginase 1 expression supporting their suppressive phenotype. Moreover, suppressive $Ly6C^{int}$ $Ly6G^+$ myeloid cells, called PMN-MDSC are known to participate to tumor cell transformation and dissemination.[30-32] In Ret mice, we previously demonstrated that PMN-MDSC infiltrating the primary tumor drive tumor cell dissemination by inducing an epithelial-mesenchymal transition.[19] Interestingly, we now show that the inactivation of IL4I1 in the same model significantly limits the presence of PMN-MDSC at the primary tumor site. This effect may, in part, contribute to delay the disease progression in RetIL4I1KO mice, as we previously observed a similar delay after specifically depleting $Ly6G^+$ cells in IL4I1 competent Ret mice.[19] It is now demonstrated that $\gamma\delta$ T cells contribute to the recruitment of PMN-MDSC in hepatocellular carcinoma, colon, breast or ovarian cancers via their ability to produce IL-17 (reviewed in ref. [20]). Our recent data showed that the genetic inactivation of iNOS also significantly impaired the recruitment

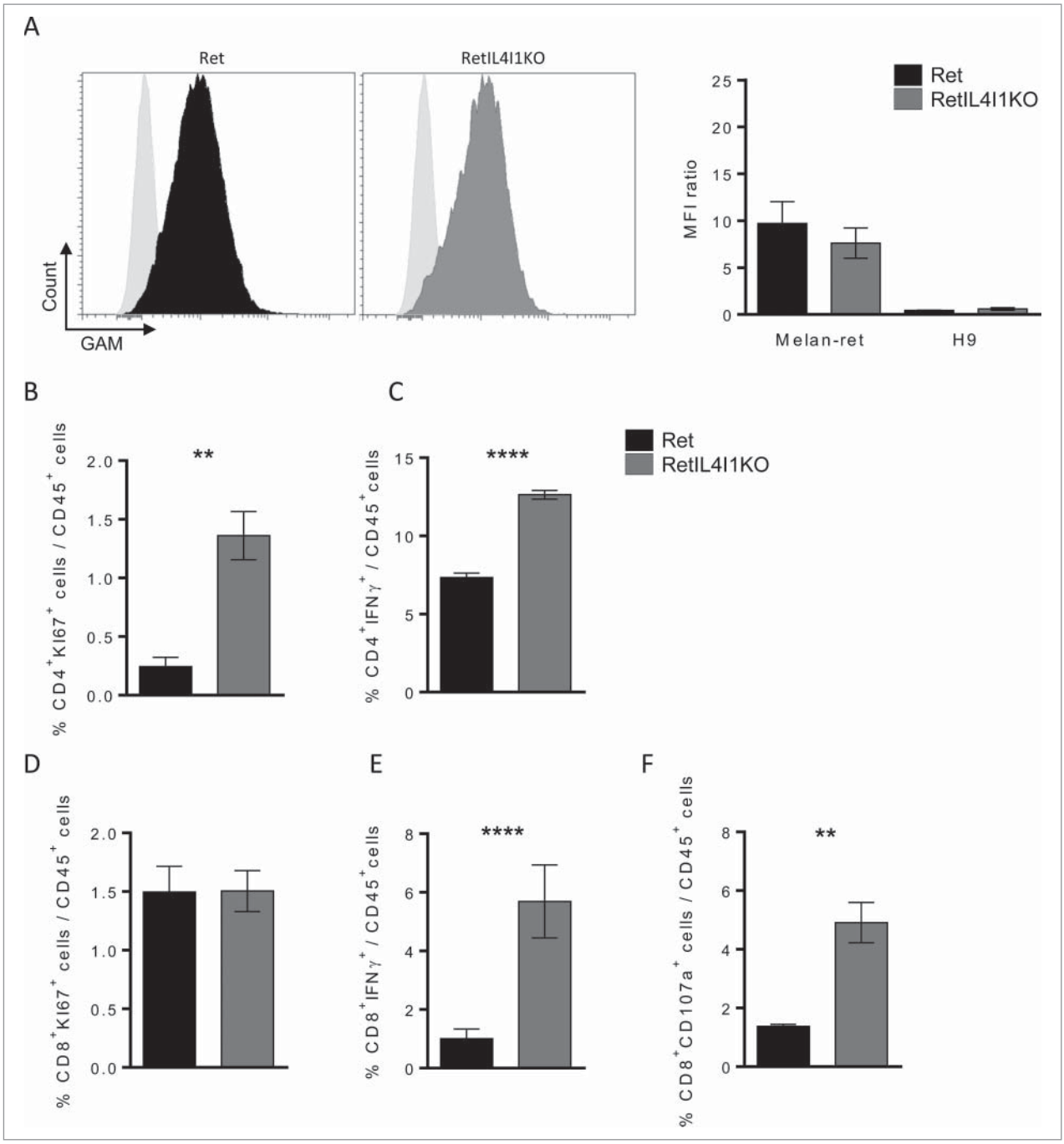

Figure 4. IL4I1 deficiency improves anti-tumor properties of $CD4^+$ and $CD8^+$ T cells, but not the generation of tumor-specific antibodies. (A) Flow-cytometric analysis of the presence of antitumor antibodies in the sera of 3-mo old Ret and RetIL4I1KO mice. (Left) Representative histograms (light gray, staining with the secondary antibody alone; black, Ret mice serum; dark gray, RetIL4I1KO mice serum), (right) MFI ratios were calculated by dividing the MFI obtained with a given serum by the MFI obtained with the secondary antibody. (B-F) Frequency (%) of $CD4^+$ or $CD8^+$ T cells expressing KI67 (B and D) or IFNγ (Cand E) and the proportion of $CD8^+$ $CD107a^+$ within the primary tumor. Graphs depict the mean ± SEM from at least two independent experiments. $^{**}p < 0.01$; $^{****}p < 0.00001$.

of PMN-MDSC within the primary melanoma in Ret mice and that iNOS potentiated the accumulation of IL-17 producing $\gamma\delta$ T cells leading to PMN-MDSC recruitment.[21] In the present work, we did not evidence a significant difference of tumor infiltrating $\gamma\delta$ T cells between Ret and RetIL4I1KO mice suggesting that a $\gamma\delta$ T cell-independent mechanism is involved in IL4I1-mediated PMN-MDSC recruitment.

The ratio between $Ly6C^{int}$ $Ly6G^+$ cells and T lymphocytes has been reported to be essential to control outcomes in several types of cancer.[22,23] In RetIL4I1KO mice, we observed a significant enhancement of the proportion of B and T lymphocytes within the primary tumor when compared with Ret mice. B cell accumulation may have led to their activation and differentiation into cells secreting tumor reactive antibodies. However, our data indicate that the plasma cell frequency in lymphoid organs and the level of tumor-specific antibodies were comparable between Ret and RetIL4I1KO mice. Despite this absence of difference in the humoral response, the increased B cell infiltration of the RetIL4I1KO tumors may improve the antitumor response, as it has been observed in

Table 2. Patients and melanoma characteristics.

Characteristics	Patients ($n = 20$)
Gender	Female : 45% ($n = 9$)
	Male : 55% ($n = 11$)
Age (Years) (Median and range)	58 (32–85)
Histological type	ALM : 25% ($n = 5$)
	NM : 45% ($n = 9$)
	SSM : 30% ($n = 6$)
Stages	IIA : 25% ($n = 5$)
	IIB : 15% ($n = 3$)
	IIC : 15% ($n = 3$)
	IIIA : 30% ($n = 6$)
	IIIB : 15% ($n = 3$)
IL4I1 density	< Median : 45% ($n = 9$)
Median : 22 cells/mm^2	> Median : 55% ($n = 11$)

ALM: Acral lentiginous melanoma; NM: Nodular melanoma.
SSM: Superficial spreading melanoma.

melanoma patients that the B cell infiltration correlates with a higher number of activated T cells and a better outcome.[24,25]

We previously reported that IL4I1 inhibits tumor specific T cells in a model of B16 melanoma cells expressing ectopically IL4I1.[11] We confirm and extend these results by showing that tumor infiltrating CD4$^+$ and CD8$^+$ T cells are more numerous and exhibit respectively higher Th1 and cytotoxic properties in RetIL4I1KO mice than in Ret mice. More importantly, CD8$^+$ T cells are less frequent in primary tumors from melanoma patients enriched in IL4I1$^+$ cells.

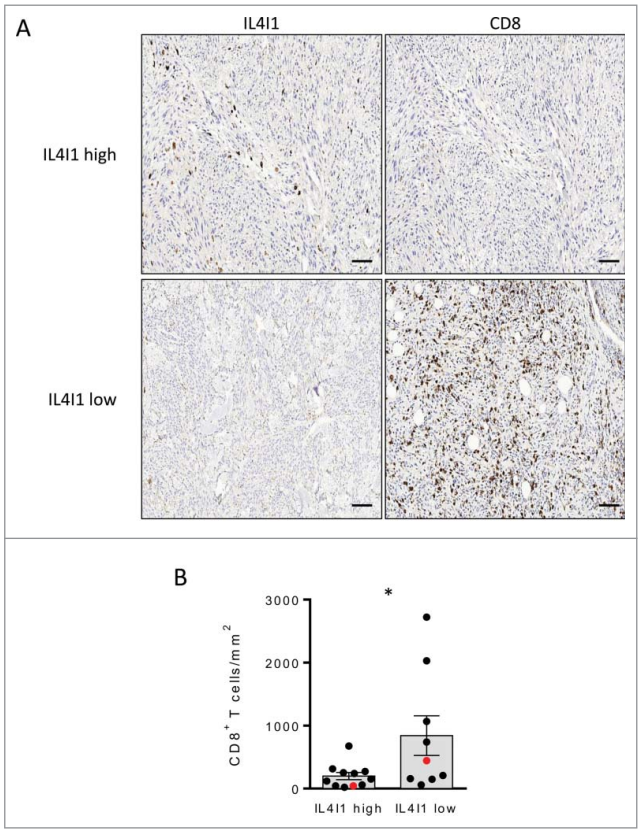

Figure 5. Primary tumors poorly infiltrated by IL4I1$^+$ cells exhibit an enhanced density of CD8$^+$ T cells in melanoma patients (A) Representative stainings of CD8$^+$ and IL4I1$^+$ cells infiltrating melanoma tumors. Scale bar, 100 μm. (B) Quantifications of CD8$^+$ T cell density in low ($n = 9$) or high ($n = 11$) IL4I1-infiltrated tumors (corresponding to < or > of the median value of IL4I1$^+$ cell density). Each point corresponds to a primary tumor. Red symbols display the representative images in A. Bars depict mean ± SEM. Unpaired *t* test; $^*p < 0.05$.

These data support a role of IL4I1 in limiting the CD8$^+$ T cell infiltrate as observed in the Ret model that may dampen the anti-melanoma response.

Our previous studies established a role for Treg in melanoma progression in Ret mice[26] and for IL4I1 in the polarization of naive CD4$^+$ T cells into Treg *in vitro*.[8] However, the similar frequency of Treg observed in the tumor draining LNs of RetIL4I1KO mice in comparison with Ret mice suggests that IL4I1 is not involved in Treg accumulation.

Overall, we have shown that the absence of IL4I1 delays tumor progression in Ret mice, *via* a reduced accumulation of PMN-MDSC at the primary tumor site, accompanied by an enhanced accumulation of antitumor Th1 and cytotoxic T cells. Thus, our results bring new insights into the suppressive function of the IL4I1 enzyme that supports tumor escape by altering the tumor immune microenvironment. The reduced CD8$^+$ T cell infiltrate, observed in IL4I1-enriched human primary melanomas, strengthens the rationale for the development of novel therapies targeting IL4I1.

Materials and methods

Mice and cell lines

Mice deficient for IL4I1 gene (IL4I1KO) were purchased from Taconic with 129/B6 background and developed by Drs. F. Castellano and V. Molinier-Frenkel on a C57BL/6J genetic background at the TAAM (Orleans, France). C57BL/6J littermates were used as WT controls. MT/ret$^{+/-}$ transgenic mice (designated as Ret) generated on the C57BL/6J background expressed heterozygously the human RET oncogene. Ret mice were crossed with IL4I1KO mice to obtain RetIL4I1KO mice. Clinical signs of mice were assessed once a week. Three- to six-month old mice were used for experiments. Mice were killed at indicated times. All mice were maintained in our animal facility under specific pathogen-free conditions.

The B16-F10 melanoma cell line provided by Pr. I. Fidler (University of Texas M.D. Anderson Cancer Center, Houston, TX) was cultured in RPMI 1640+Glutamax (Gibco®), 10% fetal calf serum, 100 U mL^{-1} penicillin and streptomycin at 37°C, 5% CO_2. 10^6 B16-F10 cells were inoculated s.c into the flank or i.v of 10-week old WT or IL4I1KO mice. Lungs were removed two weeks after tumor inoculation for colony counts.

Human biopsies characteristics

Cutaneous primary melanoma samples were obtained from patients were collected in Cochin hospital (Paris, France). Patients were included if the size of the primary tumor was large enough to allow both an adequate pathological analysis and to spare a fresh tumor sample for the research program. Patient characteristics are described in Table 2.

Single cell suspension procedures

LNs and spleen were mechanically dissociated, homogenized and passed through a nylon cell strainer (BD Falcon) in 5%

fetal calf serum and 0.5% EDTA in phosphate-buffered saline (PBS). Primary tumors were mechanically dissociated and digested with 1 mg mL^{-1} collagenase A and 0.1 mg mL^{-1} DNase I (Roche, Germany) for 20 min 37°C.

Flow cytometry and antibodies

After blocking Fc receptors using anti-CD16/32 antibodies, cells were stained with the appropriate combination of the following antibodies: CD45.2 (104), CD19 (1D3), B220 (RA3–6B2), CD138 (281–2), CD11c (HL3), CD11b (M1/70), NK1.1 (PK136), Ly6G (1A8), Ly6C (AL-21), CD8 (53–6.7), CD4 (RM 4–5), TCRβ (H57–597), TCRδ (GL3), CD107a (1D4B) that were purchased from BD Biosciences except anti-CD11b from eBioscience. The transcription factor staining Buffer Set (eBioscience) was used for the Ki67 (B56) and FOXP3 (150D) staining. IFNγ (XMG1.2) staining was performed after stimulation of single cell suspensions with Phorbol 12-myristate 13-acetate (PMA) (50 ng mL^{-1}) (Sigma), ionomycin (0.5 μg mL^{-1}) (Sigma) and 1 μL mL^{-1} Golgi PlugTM (BD Biosciences) for 4 h at 37°C 5% CO_2. Cells were incubated with Live/Dead Far red stain (Invitrogen), according to the manufacturer protocol before Ab surface staining. Then, intracellular staining was performed using Cytofix/CytopermTM kit (BD Biosciences) following the manufacturer's instructions.

Data were acquired on LSR Fortessa (BD) and analyzed with Diva software (BD Biosciences). Data acquisition was performed on the Cochin Immunobiology facility.

Tumor-specific antibody assay

Sera from Ret and RetIL4I1KO mice were obtained following intracardiac blood collection. Melan-Ret cell line (derived from a cutaneous tumor from a Ret mouse,[15] and H9 cells (American Type Culture Collection) were incubated with purified anti-CD16/32 Ab. Cells were incubated with or without sera and then stained with Alexa Fluor 647-conjugated Goat anti-mouse κ (GAM) from Invitrogen to reveal melanoma specific antibodies. Data are expressed using MFI ratio between serum+GAM condition and GAM alone.

Histological stainings and microscopy

Primary tumor samples from Ret and RetIL4I1KO mice were fixed in paraformaldehyde overnight and then embedded in paraffin. 4 μm sections of blocks were cut using a microtome (Leica, Germany) and mounted on slides (Superfrost plus, Menzel Glaser, Germany). For immunostainings, slides were deparaffinized in four washes of Ultraclear (VWR, Switzerland) for 5 min each followed by four washes of 3 min each in 100% ethanol. Slides were then rinsed in distilled water. Heat induced epitope retrieval in citrate buffer pH6 was performed before staining with antibodies against CD34 (EP373Y). Image acquisition was done on SP5 confocal microscope (Leica, Germany) using stacks of images through the whole section. Vessel density was measured as the CD34 staining area to total tumor area ratio using imageJ software (NIH, USA). For human staining, sections of 4 μm thickness were obtained from biopsies of primary melanoma embedded in paraffin at Curie Institute (Pr. A. Salomon, Paris, France). After paraffin removal, antigen retrieval and peroxidase blockade, non-specific reactivity was performed with incubation of PBS, 1% BSA for 20 min at room temperature (RT). Primary Abs Rabbit anti-IL4I1 or Mouse anti-$CD8^+$ (4B11, DAKO) were incubated 30 min at RT. Then, slides were incubated with the appropriate DAB-conjugated secondary Ab for 30 min at RT and DAB substrate was added for 10 min. The whole procedure was performed on fully automated stainer Leica-Bond-III (Leica Biosystems, Germany). Finally, nuclei were colored with hematoxylin and slides were mounted in Vectashield mounting medium (Vector Labs). Images were acquired using an automated high-resolution scanning system (Lamina^{TM}, PerkinElmer) with 20X objective. Acquisitions were performed with Lamina software and images were analyzed with ImageJ and Panoramic Viewer (3DHISTECH).

IL4I1 activity measurements

10^5 cells were lysed in PBS containing protease inhibitors (Complete mini, Roche). The IL4I1 activity was determined in cell lysates, as described previously.[2] The release of H_2O_2 was measured in presence or not of 10 mM of L-Phe during 3-h incubation at 37°C with peroxidase and Amplex-Red as an indirect revelation system. Specific IL4I1 activity was calculated by subtracting the release of H_2O_2 without L-Phe from that obtained with L-Phe.

Protein quantifications

IL-12 was quantified in the serum using ELISA (Meso Scale Discovery) according to supplier instructions.

Quantitative RT-PCR

Total RNA was isolated from purified $CD11b^+$ or $CD11b^-$ cells using RNA later and RNeasy columns (Qiagen). RNA was reverse transcribed with SuperScript^{TM} II (Invitrogen) and oligo-dT18 primers. Quantitative PCR was performed using fast SYBR Green Master Mix (Applied Biosystems) and a real time PCR system (Light Cycler 1.5, Roche Diagnostics) according to standard PCR conditions. For quantitative calculations, values were normalized to GAPDH expression. IL4I1 primer sequences are the following: sens: 5′ GCA TAC GCT TCT GGA ATA CCT 3′; antisens: 5′ AAG CCC TCC TCG GAC AT 3′.

Tumor cell growth assay

B16-F10 cell growth was measured using the xCELLigence System (Roche) as described previously in ref. [18]. Briefly, 5×10^4 B16 cells were seeded into wells of E-plates. After adhesion of tumor cells (4 h), 1.5 to 150 ng per mL of recombinant murine IL4I1 (rIL4I1) (R&D system) were added to the cultures. Tumor cell proliferation was dynamically monitored every 30 min for up 40 h. Results showing normalized cell index were analyzed with the RTCA Software.

Statistics

Data are expressed as mean ± SEM. ($^{*}p < 0.05$; $^{**}p < 0.01$; $^{***}p < 0.001$). All statistical analyses were performed with Prism 5 software (GraphPad softwares) using either the Mann–Whitney *t* test or unpaired two-tailed *t* test for significance.

Study approval

Mice experiments were carried out in accordance with the guidelines of the French Veterinary Department and were approved by the Paris-Descartes Ethical Committee for Animal Experimentation (decision CEEA34.AB.038.12).

The study protocol was approved by the ethics committee CPP Ile de France III (N°Am5937–3–2834) (EUDRACT 2010-A00838–31) and the study was performed according to the Declaration of Helsinki Principles. Patients who had to be treated surgically for a primary melanoma were informed of the objectives of the study and signed a written consent before inclusion.

Disclosure of potential conflicts of interest

No potential conflicts of interest were disclosed.

Acknowledgments

L. Bod was supported by Paris V University. J-P. Ramspott was supported by a fellowship from the Claussen-Simon-Stiftung, Hamburg and an ERASMUS fellowship. This work was supported by Gefluc, Comité "Ile de France" Ligue contre le Cancer and by the Fondation ARC for cancer research. We are grateful to Y. Richard for helpful discussion, L. Douguet for critical review of the manuscript and M. Garcette for technical support. We acknowledge the Cochin cytometry and Immunobiology facility, Histology and Immunostaining facility and the Animal core facility. We thank F. Boitier, N. Kramkimel and J. Chanal for patient recruitment, the anatomopathology department of Curie Institute for the biopsies, patients who gave their consent to participate to this study, and C. Auger and D. Bourgeois from URC Paris Center who contributed to the immumela project.

Author contributions

L.B., R.L., L.W., and JP.R. did experiments; L.B., and A.P.B. designed the study with the help of V.MF., F.C. and M.F.A. L.B., V.MF., F.C and A.P.B. wrote the manuscript. All authors critically reviewed the manuscript.

References

1. Murray PJ. Amino acid auxotrophy as a system of immunological control nodes. Nature immunology 2016; 17:132-9; PMID:26784254; http://dx.doi.org/10.1038/ni.3323
2. Carbonnelle-Puscian A, Copie-Bergman C, Baia M, Martin-Garcia N, Allory Y, Haioun C, Crémades A, Abd-Alsamad I, Farcet JP, Gaulard P et al. The novel immunosuppressive enzyme IL4I1 is expressed by neoplastic cells of several B-cell lymphomas and by tumor-associated macrophages. Leukemia 2009; 23:952-60; PMID: 19436310; http://dx.doi.org/10.1038/leu.2008.380
3. Copie-Bergman C, Boulland ML, Dehoulle C, Moller P, Farcet JP, Dyer MJ, Haioun C, Roméo PH, Gaulard P, Leroy K. Interleukin 4-induced gene 1 is activated in primary mediastinal large B-cell lymphoma. Blood 2003; 101:2756-61; PMID: 12446450; http://dx.doi.org/10.1182/blood-2002-07-2215
4. Finak G, Bertos N, Pepin F, Sadekova S, Souleimanova M, Zhao H, Chen H, Omeroglu G, Meterissian S, Omeroglu A et al. Stromal gene expression predicts clinical outcome in breast cancer. Nature medicine 2008; 14:518-27; PMID: 18438415; http://dx.doi.org/10.1038/nm1764
5. Romagnani S. IL4I1: Key immunoregulator at a crossroads of divergent T-cell functions. European journal of immunology 2016; 46:2302-5; PMID: 27726138; http://dx.doi.org/10.1002/eji.201646617
6. Boulland ML, Marquet J, Molinier-Frenkel V, Moller P, Guiter C, Lasoudris F, Copie-Bergman C, Baia M, Gaulard P, Leroy K et al. Human IL4I1 is a secreted L-phenylalanine oxidase expressed by mature dendritic cells that inhibits T-lymphocyte proliferation. Blood 2007; 110:220-7; PMID: 17356132; http://dx.doi.org/10.1182/blood-2006-07-036210
7. Marquet J, Lasoudris F, Cousin C, Puiffe M, Martin-Garcia N, Baud V, Chereau F, Farcet JP, Molinier-Frenkel V, Castellano F. Dichotomy between factors inducing the immunosuppressive enzyme IL4I1 in B lymphocytes and mononuclear phagocytes. European Journal of Immunology 2010; 40:2557-68; PMID: 20683900; http://dx.doi.org/10.1002/eji.201040428
8. Cousin C, Aubatin A, Le Gouvello S, Apetoh L, Castellano F, Molinier-Frenkel V. The immunosuppressive enzyme IL4I1 promotes FoxP3(+) regulatory T lymphocyte differentiation. European journal of immunology 2015; 45:1772-82; PMID: 25778793; http://dx.doi.org/10.1002/eji.201445000
9. Yue Y, Huang W, Liang J, Guo J, Ji J, Yao Y, Zheng M, Cai Z, Lu L, Wang J. IL4I1 Is a Novel Regulator of M2 Macrophage Polarization That Can Inhibit T Cell Activation via L-Tryptophan and Arginine Depletion and IL-10 Production. PloS one 2015; 10:e0142979; PMID: 26599209; http://dx.doi.org/10.1371/journal.pone.0142979
10. Santarlasci V, Maggi L, Mazzoni A, Capone M, Querci V, Rossi MC, Beltrame L, Cavalieri D, De Palma R, Liotta F et al. IL-4-induced gene 1 maintains high Tob1 expression that contributes to TCR unresponsiveness in human T helper 17 cells. European journal of immunology 2014; 44:654-61; PMID: 24307243; http://dx.doi.org/10.1002/eji.201344047
11. Lasoudris F, Cousin C, Prevost-Blondel A, Martin-Garcia N, Abd-Alsamad I, Ortonne N, Farcet JP, Castellano F, Molinier-Frenkel V. IL4I1: an inhibitor of the CD8(+) antitumor T-cell response in vivo. European journal of immunology 2011; 41:1629-38; PMID: 21469114; http://dx.doi.org/10.1002/eji.201041119
12. Kato M, Takahashi M, Akhand AA, Liu W, Dai Y, Shimizu S, Iwamoto T, Suzuki H, Nakashima I. Transgenic mouse model for skin malignant melanoma. Oncogene 1998; 17:1885-8; PMID: 9778055; http://dx.doi.org/10.1038/sj.onc.1202077
13. Eyles J, Puaux AL, Wang X, Toh B, Prakash C, Hong M, Tan TG, Zheng L, Ong LC, Jin Y et al. Tumor cells disseminate early, but immunosurveillance limits metastatic outgrowth, in a mouse model of melanoma. The Journal of clinical investigation 2010; 120:2030-9; PMID: 20501944; http://dx.doi.org/10.1172/JCI42002
14. Lengagne R, Graff-Dubois S, Garcette M, Renia L, Kato M, Guillet JG, Engelhard VH, Avril MF, Abastado JP, Prévost-Blondel A. Distinct role for CD8 T cells toward cutaneous tumors and visceral metastases. Journal of immunology 2008; 180:130-7; PMID:18097012; http://dx.doi.org/10.4049/jimmunol.180.1.130
15. Lengagne R, Le Gal FA, Garcette M, Fiette L, Ave P, Kato M, Briand JP, Massot C, Nakashima I, Rénia L et al. Spontaneous vitiligo in an animal model for human melanoma: role of tumor-specific CD8+ T cells. Cancer research 2004; 64:1496-501; PMID: 14973052; http://dx.doi.org/10.1158/0008-5472.CAN-03-2828
16. Ananieva E. Targeting amino acid metabolism in cancer growth and anti-tumor immune response. World journal of biological chemistry 2015; 6:281-9; PMID: 26629311; http://dx.doi.org/10.4331/wjbc.v6.i4.281
17. Bronte V, Brandau S, Chen SH, Colombo MP, Frey AB, Greten TF, Mandruzzato S, Murray PJ, Ochoa A, Ostrand-Rosenberg S et al. Recommendations for myeloid-derived suppressor cell nomenclature and characterization standards. Nature communications 2016; 7:12150; PMID: 27381735; http://dx.doi.org/10.1038/ncomms12150
18. Lengagne R, Pommier A, Caron J, Douguet L, Garcette M, Kato M, Avril MF, Abastado JP, Bercovici N, Lucas B et al. T cells contribute to tumor progression by favoring pro-tumoral properties of intratumoral myeloid cells in a mouse model for spontaneous melanoma.

PloS one 2011; 6:e20235; PMID: 21633700; http://dx.doi.org/10.1371/journal.pone.0020235

19. Toh B, Wang X, Keeble J, Sim WJ, Khoo K, Wong WC, Kato M, Prevost-Blondel A, Thiery JP, Abastado JP. Mesenchymal transition and dissemination of cancer cells is driven by myeloid-derived suppressor cells infiltrating the primary tumor. PLoS biology 2011; 9:e1001162; PMID: 21980263; http://dx.doi.org/10.1371/journal.pbio.1001162
20. Rei M, Pennington DJ, Silva-Santos B. The emerging Protumor role of gammadelta T lymphocytes: implications for cancer immunotherapy. Cancer research 2015; 75:798-802; PMID: 25660949; http://dx.doi.org/10.1158/0008-5472.CAN-14-3228
21. Douguet L, Bod L, Lengagne R, Labarthe L, Kato M, Avril M-F, Prévost-Blondel A. Nitric oxide synthase 2 is involved in the protumorigenic potential of $\gamma\delta$17 T cells in melanoma. Oncoimmunology 2016; 5:e1208878; PMID: 27622078; http://dx.doi.org/10.1080/2162402X.2016.1208878
22. Koh CH, Bhoo-Pathy N, Ng KL, Jabir RS, Tan GH, See MH, Jamaris S, Taib NA. Utility of pre-treatment neutrophil-lymphocyte ratio and platelet-lymphocyte ratio as prognostic factors in breast cancer. British journal of cancer 2015; 113:150-8; PMID: 26022929; http://dx.doi.org/10.1038/bjc.2015.183
23. Ferrucci PF, Gandini S, Battaglia A, Alfieri S, Di Giacomo AM, Giannarelli D, Cappellini GC, De Galitiis F, Marchetti P, Amato G et al. Baseline neutrophil-to-lymphocyte ratio is associated with outcome of ipilimumab-treated metastatic melanoma patients. British journal of cancer 2015; 112:1904-10; PMID: 26010413; http://dx.doi.org/10.1038/bjc.2015.180
24. Garg K, Maurer M, Griss J, Bruggen MC, Wolf IH, Wagner C, Willi N, Mertz KD, Wagner SN. Tumor-associated B cells in cutaneous primary melanoma and improved clinical outcome. Human pathology 2016; 54:157-64; PMID: 27107457; http://dx.doi.org/10.1016/j.humpath.2016.03.022
25. Ladanyi A, Kiss J, Mohos A, Somlai B, Liszkay G, Gilde K, Fejös Z, Gaudi I, Dobos J, Tímár J. Prognostic impact of B-cell density in cutaneous melanoma. Cancer immunology, immunotherapy : CII 2011; 60:1729-38; PMID: 21779876; http://dx.doi.org/10.1007/s00262-011-1071-x
26. Pommier A, Audemard A, Durand A, Lengagne R, Delpoux A, Martin B, Douguet L, Le Campion A, Kato M, Avril MF et al. Inflammatory monocytes are potent antitumor effectors controlled by regulatory CD4+ T cells. Proceedings of the National Academy of Sciences of the United States of America 2013; 110:13085-90; PMID: 23878221; http://dx.doi.org/10.1073/pnas.1300314110
27. Gabrilovich DI, Ostrand-Rosenberg S, Bronte V. Coordinated regulation of myeloid cells by tumours. Nature reviews Immunology 2012; 12:253-68.
28. Umansky V, Sevko A, Gebhardt C, Utikal J. Myeloid-derived suppressor cells in malignant melanoma. Journal der Deutschen Dermatologischen Gesellschaft = Journal of the German Society of Dermatology: JDDG 2014; 12:1021-7.
29. Ostrand-Rosenberg S. Myeloid-derived suppressor cells: more mechanisms for inhibiting antitumor immunity. Cancer immunology, immunotherapy: CII 2010; 59:1593-600.
30. Dong C, Slattery MJ, Liang S, Peng HH. Melanoma cell extravasation under flow conditions is modulated by leukocytes and endogenously produced interleukin 8. Molecular & cellular biomechanics: MCB 2005; 2:145-59.
31. Slattery MJ, Dong C. Neutrophils influence melanoma adhesion and migration under flow conditions. International journal of cancer Journal international du cancer 2003; 106:713-22.
32. Hoskins MH, Dong C. Kinetics analysis of binding between melanoma cells and neutrophils. Molecular & cellular biomechanics: MCB 2006; 3:79-87.